



Probabilistically shaped PDM 4096-QAM transmission over up to 200 km of fiber using standard intradyne detection

SAMUEL L.I. OLSSON,^{1,*} JUNHO CHO,¹ SETHUMADHAVAN CHANDRASEKHAR,¹ XI CHEN,¹ PETER J. WINZER,¹ AND SERGEJS MAKOVEJS²

¹Nokia Bell Labs, Holmdel, New Jersey, 07733, USA

²Corning Optical Communications, Ewloe, CH5 3XD, UK

*samuel.olsson@nokia-bell-labs.com

Abstract: We demonstrate transmission of a probabilistically shaped polarization-division multiplexed 3-GBd 4096-QAM signal over up to 200 km of backward Raman amplified Corning® Vascade® EX2000 fiber. The 3-GBd signal with a root-raised-cosine roll-off of 0.01 has the potential to generate a spectral efficiency of 19.77 bit/s/Hz over 50 km of fiber.

© 2018 Optical Society of America under the terms of the [OSA Open Access Publishing Agreement](#)

OCIS codes: (060.1660) Coherent communications; (060.2330) Fiber optics communications.

References and links

1. P. J. Winzer, "Energy-efficient optical transport capacity scaling through spatial multiplexing," *IEEE Photonics Technol. Lett.* **23**, 851–853 (2011).
2. P. Dong, X. Liu, S. Chandrasekhar, L. L. Buhl, R. Aroca, and Y.-K. Chen, "Monolithic silicon photonic integrated circuits for compact 100+ Gb/s coherent optical receivers and transmitters," *IEEE J. Sel. Top. Quantum Electron.* **20**, 6100108 (2014).
3. N. Eiselt, J. Wei, H. Griesser, A. Dochhan, M. H. Eiselt, J.-P. Elbers, J. J. V. Olmos, and I. T. Monroy, "Evaluation of real-time 8×56.25 Gb/s (400G) PAM-4 for inter-data center application over 80 km of SSMF at 1550 nm," *J. Lightwave Technol.* **35**, 955–962 (2017).
4. M.-F. Huang, D. Qian, and E. Ip, "50.53-Gb/s PDM-1024QAM-OFDM transmission using pilot-based phase noise mitigation," in *Optoelectronics and Communications Conference (OECC)* (2011).
5. Y. Koizumi, K. Toyoda, M. Yoshida, and M. Nakazawa, "1024 QAM (60 Gbit/s) single-carrier coherent optical transmission over 150 km," *Opt. Express* **20**, 12508–12514 (2012).
6. D. Qian, E. Ip, M.-F. Huang, M.-J. Li, and T. Wang, "698.5-Gb/s PDM-2048QAM transmission over 3km multicore fiber," in *European Conference and Exhibition on Optical Communication (ECOC)* (2013), paper Th.1.C.5.
7. S. Beppu, K. Kasai, M. Yoshida, and M. Nakazawa, "2048 QAM (66 Gbit/s) single-carrier coherent optical transmission over 150 km with a potential SE of 15.3 bit/s/Hz," *Opt. Express* **23**, 4960–4969 (2015).
8. Q. Chen, J. He, R. Deng, M. Chen, and L. Chen, "FFT-size efficient 4096-QAM OFDM for low-cost DML-based IMDD system," *IEEE Photonics J.* **8**, 7804010 (2016).
9. F. Buchali, F. Steiner, G. Böcherer, L. Schmalen, P. Schulte, and W. Idler, "Rate adaptation and reach increase by probabilistically shaped 64-QAM: An experimental demonstration," *J. Lightwave Technol.* **34**, 1599–1609 (2016).
10. M. P. Yankov, F. Da Ros, E. P. da Silva, S. Forchhammer, K. J. Larsen, L. K. Oxenløwe, M. Galili, and D. Zibar, "Constellation shaping for WDM systems using 256QAM/1024QAM with probabilistic optimization," *J. Lightwave Technol.* **34**, 5146–5156 (2016).
11. S. Chandrasekhar, B. Li, J. Cho, X. Chen, E. C. Burrows, G. Raybon, and P. J. Winzer, "High-spectral-efficiency transmission of PDM 256-QAM with parallel probabilistic shaping at record rate-reach trade-offs," in *European Conference and Exhibition on Optical Communication (ECOC)* (2016), paper Th.3.C.1.
12. W. Idler, F. Buchali, L. Schmalen, E. Lach, R.-P. Braun, G. Böcherer, P. Schulte, and F. Steiner, "Field demonstration of 1 Tbit/s super-channel network using probabilistically shaped constellations," in *European Conference and Exhibition on Optical Communication (ECOC)* (2016), paper M1.D.2.
13. J. Cho, X. Chen, S. Chandrasekhar, G. Raybon, R. Dar, L. Schmalen, E. Burrows, A. Adamiecki, S. Corteselli, Y. Pan, D. Correa, B. McKay, S. Zsigmond, P. Winzer, and S. Grubb, "Trans-atlantic field trial using high spectral efficiency probabilistically shaped 64-QAM and single-carrier real-time 250-Gb/s 16-QAM," *J. Lightwave Technol.* (to be published).
14. G. Böcherer, F. Steiner, and P. Schulte, "Bandwidth efficient and rate-matched low-density parity-check coded modulation," *IEEE Trans. Commun.* **63**, 4651–4665 (2015).

15. G. Böcherer, "Achievable rates for probabilistic shaping," ArXiv preprint, 2017. [Online]. Available: <https://arxiv.org/abs/1707.01134v4>.
16. J. Cho and L. Schmalen, "Construction of protographs for large-girth structured LDPC convolutional codes," in *IEEE International Conference on Communications (ICC)* (2015).
17. J. Cho, L. Schmalen, and P. Winzer, "Normalized generalized mutual information as a forward error correction threshold for probabilistically shaped QAM," in *European Conference and Exhibition on Optical Communication (ECOC)* (2017), paper M.2.D.
18. A. Alvarado, E. Agrell, D. Lavery, R. Maher, and P. Bayvel, "Replacing the soft-decision FEC limit paradigm in the design of optical communication systems," *J. Lightwave Technol.* **33**, 4338–4352 (2015).
19. T. Fehenberger, A. Alvarado, G. Böcherer, and N. Hanik, "On probabilistic shaping of quadrature amplitude modulation for the nonlinear fiber channel," *J. Lightwave Technol.* **34**, 5063–5073 (2016).

1. Introduction

The enormous growth in the number and size of distributed data centers requires data center interconnect (DCI) solutions with multi-Petabit/s point-to-point capacities at a reach of up to ~100 km of fiber. The most cost-effective and power-efficient way to satisfy such DCI needs relies on technology-specific trade-offs between modulation and detection complexity, wavelength division multiplexed (WDM) system bandwidth, and number of parallel spatial paths [1]. For a given transponder technology and complexity, amortizing transponder costs over as many bits/s as possible is generally a beneficial strategy. This makes tightly integrated digital coherent receivers [2] using the largest possible symbol constellation supported by the link (i.e., the highest supported spectral efficiency (SE)) an attractive candidate for high-capacity DCI systems, despite their seemingly higher complexity compared to less scalable solutions using, e.g., multi-level pulse amplitude modulation (PAM) [3]. As DCI systems are often greenfield deployments, built in connection with newly constructed data centers, they also allow for advanced fiber and amplification schemes (such as Raman amplification), if such approaches result in overall lower-cost and lower-energy solutions. While our goal is not to make techno-economic statements in this work, we examine the extreme end of possible future DCI system trade-offs, pushing SEs over advanced, Raman-amplified fiber to their limits.

Most system demonstrations using higher-order quadrature amplitude modulation (QAM) are based on a single optical channel, which allows an estimate of the *potential* SE from the spectral roll-off of the respective formats. With the root-raised-cosine (RRC) roll-off factor denoted by ρ , the potential SE is calculated as the ratio between the bit rate R_b and the symbol rate R_s multiplied by $1 + \rho$, i.e., the potential SE equals $R_b / [(1 + \rho)R_s]$. Record results for the potential SE in short-reach optical communications using uniform QAM formats of very high order are summarized in Fig. 1. Uniform 1024-QAM has been demonstrated over a transmission distance of 160 km in an orthogonal frequency-division multiplexing (OFDM) system at a potential SE of 11.7 bit/s/Hz and a net bit rate of 40.42 Gb/s [4], and over 150 km in a single-carrier system at a potential SE of 13.8 bit/s/Hz and a net bit rate of 55.8 Gb/s [5]. Uniform 2048-QAM has been transmitted over 3 km at a potential SE of 17.1 bit/s/Hz and a net bit rate of 58.2 Gb/s [6], and over 150 km at a potential SE of 15.3 bit/s/Hz and a net bit rate of 52.8 Gb/s [7], albeit with a phase recovery based on a rather complex optical phase-locked loop. Uniform 4096-QAM has been demonstrated over a distance of 10 km in a direct detection system [8], at a potential SE of only 9.5 bit/s/Hz and a net bit rate of 9.5 Gb/s. Probabilistically shaped (PS) QAM has been demonstrated to achieve record-high SEs in several lab experiments [9–11], and field trials [12, 13], due to its flexible rate adaptability and its near-optimal energy efficiency [14]. However, in short-reach systems, ultra-high SE using PS QAM has not been demonstrated.

In this paper, we demonstrate transmission and digital coherent detection of polarization-division multiplexed (PDM) PS 4096-QAM over up to 200 km (4×50 km) of backward Raman amplified Vascade EX2000 fiber. Using a 3-GBd signal with an RRC roll-off of 0.01 we obtain a potential SE of 19.77 bit/s/Hz at a net bit rate of 59.89 Gb/s over 50 km of fiber (18.58 bit/s/Hz

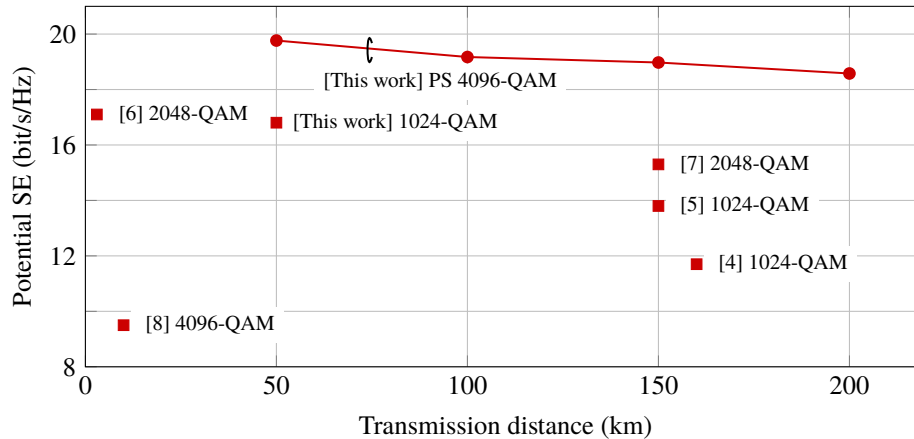


Fig. 1. Experimentally demonstrated potential SEs in short-reach systems.

at 56.29 Gb/s over 200 km), as shown in Fig. 1 (circles). Our transmitter and receiver use two independent, compact off-the-shelf ultra-narrow-linewidth lasers together with a standard opto-electronic coherent front-end and purely digital intradyne detection without the need for auxiliary optical phase or frequency locking techniques.

2. Experimental setup and DSP

A schematic of the experimental setup for ultra-high SE PS 4096-QAM transmission is shown in Fig. 2. The signal from an ultra-narrow-linewidth (1-Hz) laser (OEWaves OE4030) at 193.398 THz was amplified using an erbium-doped fiber amplifier (EDFA) and subsequently modulated with 3-GBd PS 4096-QAM data (0.01 RRC roll-off) using a 2-channel 14-bit digital-to-analog converter (DAC) (Keysight M8190A) running at 6 GS/s and an in-phase/quadrature (I/Q) modulator (Fujitsu FTM7961EX). The two DAC output signals had a voltage swing of 700 mV_{pp} and were filtered by two cascaded low-pass RF filters with cut-off frequencies of 1525 MHz (Mini-Circuits VLF-1525+) and 5000 MHz (Mini-Circuits VLF-5000+) before they were used to drive the I/Q modulator. The electrical recovered symbol signal-to-noise ratio (SNR), obtained by connecting the DAC output directly to the receiver's analog-to-digital converter (ADC) input, was measured to be 39.4 dB using a 1024-QAM signal. The data sequence consisted of 73728 randomly chosen symbols when uniform QAM was generated. The data sequence used to generate PS QAM is discussed in Section 3 below. After modulation the signal was amplified by an EDFA and launched into a PDM emulation stage implemented by dividing the signal into two copies and delaying one copy with respect to the other before recombining them on orthogonal polarizations using a polarization beam splitter (PBS). The de-correlation length was ~ 48 m (> 700 symbols at 3 GBd).

The signal was boosted by an EDFA followed by a variable optical attenuator (VOA) to adjust the launch power into the transmission link, measured at point P_{in}. The link consisted of up to four 50-km spans of Vascade EX2000 fiber with an average loss of 0.16 dB/km, dispersion of 20.1 ps/nm/km, and effective area of 112 μm². Each span was preceded by an isolator and amplified to transparency using backward Raman pumping with four pumps. The pumps were at 1424 nm with 250 mW, 1435 nm with 230 mW, 1455 nm with 200 mW, and 1466 nm with 180 mW. The optical signal-to-noise ratio (OSNR), quoted with a 0.1-nm noise reference bandwidth, of the signal launched into the transmission link was 36 dB.

At the receiver a tunable narrow-linewidth (<100-Hz) laser (NKT Koheras BASIK X15) was

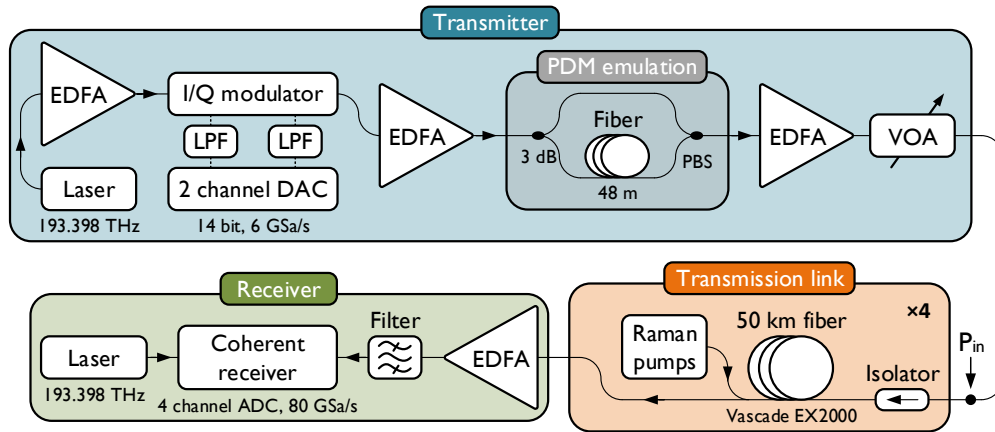


Fig. 2. Schematic of experimental setup used for PS 4096-QAM transmission. EDFA: erbium-doped fiber amplifier, DAC: digital-to-analog converter, LPF: cascade of two low-pass filters, I/Q: in-phase/quadrature, PDM: polarization-division multiplexing, PBS: polarization beam splitter, VOA: variable optical attenuator, ADC: analog-to-digital converter.

used as local oscillator for intradyne detection. After a PDM 90-degree hybrid with balanced detection (u²t PBDV2150R) the signal was sampled at 80 GSa/s over a time window of 0.1 ms (3×10^5 symbols) using a real-time oscilloscope (Keysight DSOZ634A) with 8-bit ADCs. The ADC inputs were filtered by two cascaded low-pass RF filters with cut-off frequencies of 1700 MHz (Mini-Circuits VLF-1700+) and 1525 MHz (Mini-Circuits VLF-1525+). Off-line digital signal processing (DSP) consisted of resampling to 2 samples/symbol and polarization demultiplexing using pilot-assisted pre-convergence with least-mean square (LMS) equalization followed by blind LMS equalization and blind carrier phase recovery. Timing recovery was performed through an exhaustive timing search algorithm. Only the blindly recovered data were used for subsequent performance evaluation.

3. Probabilistic shaping and FEC

Probabilistic shaping of the 4096-QAM constellation was realized by multiplexing two independent PS 64-PAM constellations of 73728 symbols each as I and Q components, using the probabilistic amplitude shaping (PAS) architecture [14]. We used the Maxwell-Boltzmann (MB) distribution for the transmitted symbol distribution, defined by the probability mass function $P(x) = \exp(-\lambda x^2) / \sum_{z \in \chi} \exp(-\lambda z^2)$, where χ is the set of M -PAM symbols ($M = 64$ for 4096-QAM). The shaping parameter is given by $\beta := H(P) - 1$, where $H(\cdot)$ denotes the entropy function, which is used in this paper to maximize the information rate of the PS 4096-QAM signal by optimal shaping. The maximum information rate supported by the PDM PS 4096-QAM constellation, termed the entropy rate, is $H = 4(1 + \beta)$ bit/symbol/2-pol, which increases linearly with β . For the constellation template of 4096-QAM, we have the range $0 \leq \beta \leq \log_2(4096)/2 - 1 = 5$, hence an arbitrary entropy rate in $4 \leq H \leq 24$ can be realized by PDM PS 4096-QAM. Note that the PAS architecture only allows for forward error correction (FEC) codes of rates larger than $(m - 1)/m$, with $m = \log_2(M)$, i.e., code rates larger than 5/6 in our situation.

The system performance that can be achieved by ideal rate-adaptable FEC is first quantified by the generalized mutual information (GMI) for bit-metric decoding (BMD) in two polarizations,

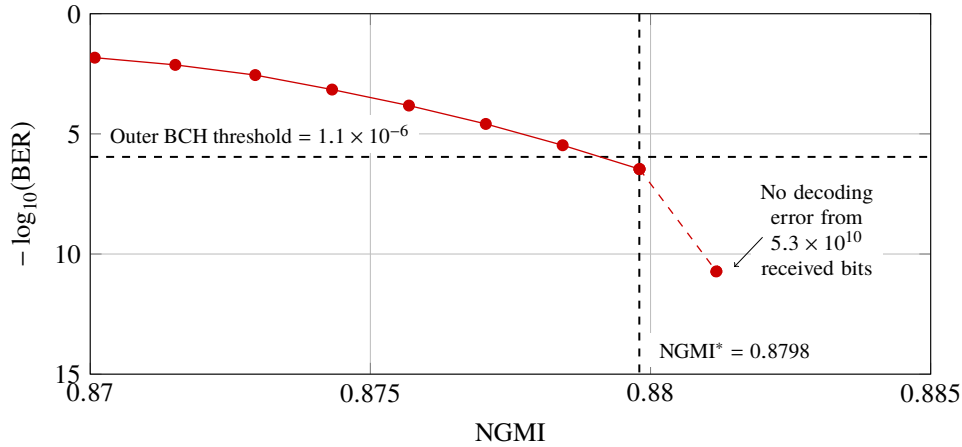


Fig. 3. Simulated post-FEC BER of rate 0.8469 SC-LDPC code versus NGMI.

which can be estimated from the received symbols as

$$\text{GMI} = H + \frac{4}{N} \sum_{k=1}^N \sum_{i=1}^m \log_2 \frac{\sum_{x \in \mathcal{X}_{b_{k,i}}} q(y_k|x)P(x)}{\sum_{x \in \mathcal{X}} q(y_k|x)P(x)} \quad [\text{bit/symbol}/2\text{-pol}], \quad (1)$$

where $b_{k,i}$ is the i -th bit of the k -th transmitted symbol, y_k is the k -th received symbol, N is the number of received symbols, and $q(y|x) = 1/\sqrt{2\pi\sigma^2} \exp[-(y-x)^2/(2\sigma^2)]$ denotes the probability density function of the received symbol y given the transmitted symbol x in the memoryless additive white Gaussian noise (AWGN) auxiliary channel of the true fiber optic channel with a one-dimensional noise variance of σ^2 . The GMI is the achievable information rate (AIR) under our bit-interleaved coded modulation (BICM). We use binary reflected Gray coding for bit labeling. Note that the GMI in its Monte Carlo estimation form, as presented in Eq. (1), has the same expression as the BMD rate of [15], while the achievable information rate in a mathematical channel model may more accurately be represented by the BMD rate in an analytic form.

For practical low-complexity fixed-rate FEC coding, we use a spatially-coupled low-density parity-check (SC-LDPC) code of code rate 0.8469 (18.08% overhead). The SC-LDPC code is constructed based on [16], by quasi-cyclically lifting a shortest-constraint-length girth-6 rate-5/6 regular variable-degree-4 protograph with a lifting factor of 94, with a small fraction of puncturing for fine tuning of the code rate. Sliding-window decoding is performed over 1000 coupled lifted protographs using a normalized min-sum algorithm with a window size of 196 without per-sliding iterations, which leads to 25 check node operations per variable node. A potential error floor of the SC-LDPC code is removed by an outer hard-decision BCH (8191, 8126, 5) code that has a bit error ratio (BER) threshold of 1.1×10^{-6} . The concatenated code rate is $0.8469 \times 8126/8191 = 0.8402$ (19.02% overhead), which fulfils the requirement of the PAS architecture for PS 4096-QAM, as mentioned above. Figure 3 shows the simulated post-FEC BER performance of our SC-LDPC code as a function of the normalized generalized mutual information (NGMI). The NGMI is a channel metric that accurately predicts the performance of soft-decision FEC for a wide range of PS QAM as well as for uniform QAM, regardless of the shaping parameter [17, 18]. The NGMI can be computed for PDM PS M^2 -QAM as [17]

$$\text{NGMI} = 1 - \frac{H - \text{GMI}}{4m}. \quad (2)$$

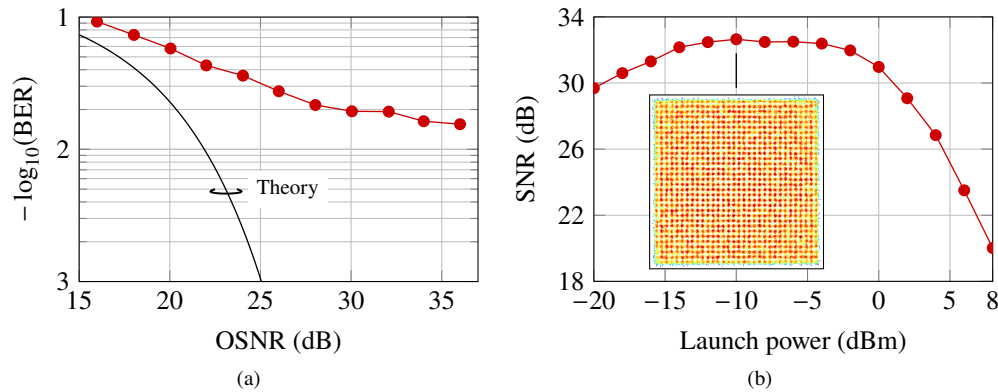


Fig. 4. (a) Measured back-to-back BER versus OSNR for 3-GBd 1024-QAM. (b) Measured SNR versus launch power for 3-GBd 1024-QAM transmission over 50-km fiber with inset showing recovered constellation diagram (x-polarization) at -10 dBm launch power.

Note that if we replace the GMI with the BMD rate on the right-hand side of Eq. (2), we arrive at the same expression as that for the achievable binary code rate of [15]. From Fig. 3, the FEC threshold of the concatenated code is found to be $NGMI^* = 0.8798$, i.e., a received $NGMI > NGMI^*$ can be decoded error-free.

While the GMI quantifies an upper bound of the information rate that is obtained with an ideal binary FEC code under BMD, the information rate that is actually achieved with a non-ideal FEC code is computed as

$$R = H - 4(1 - R_c)m \quad [\text{bit/symbol/2-pol}], \quad (3)$$

where R_c denotes the FEC code rate. For a given constellation template of size M per dimension, the second term of the right-hand side of Eq. (3) becomes constant if the FEC rate R_c is a fixed value. Therefore, following the rate adaptation approach proposed in [13], we maximize the information rate R while ensuring that FEC decoding produces error-free results by finding the maximum β (hence the maximum H) that yields a measured $NGMI$ greater than $NGMI^*$. In particular, with our FEC code of rate $R_c = 0.8402$ and a PAM size of $M = 64$, we have $R = 4\beta + 0.1643$. Taking into account an RRC roll-off factor of 0.01 for our 3-GBd signal, we obtain a potential SE of $R \times 3/3.03 = 3.9604\beta + 0.1627$ bit/s/Hz, whenever the measured $NGMI$ is greater than $NGMI^* = 0.8798$. In a realistic WDM scenario a guard band of $\sim 5\%$ of the symbol rate would typically be required [11, 13], resulting in a slightly reduced SE.

4. Results

The SE of our system was determined at transmission distances of 50 km to 200 km at a step size of 50 km by measuring the $NGMI$ versus the shaping parameter β with optimized launch power. Various prior experiments have demonstrated that the difference in optimal launch power between uniform QAM and PS QAM is negligible [9, 19], and that the optimal launch power dependence on the shaping parameter for PS QAM is weak [13]. We can therefore determine the optimal launch power for a 3-GBd 1024-QAM signal, which is easier to recover over a large range of launch powers, and then infer the optimal launch power for our PS 4096-QAM signal. Figure 4(a) shows measured back-to-back BER versus OSNR for a 3-GBd 1024-QAM signal displaying an error floor around 1.5×10^{-2} and Fig. 4(b) shows the measured SNR of the recovered constellation versus launch power for a 3-GBd 1024-QAM signal transmitted over one 50-km span. At low launch powers the signal is degraded by amplifier noise, and at high

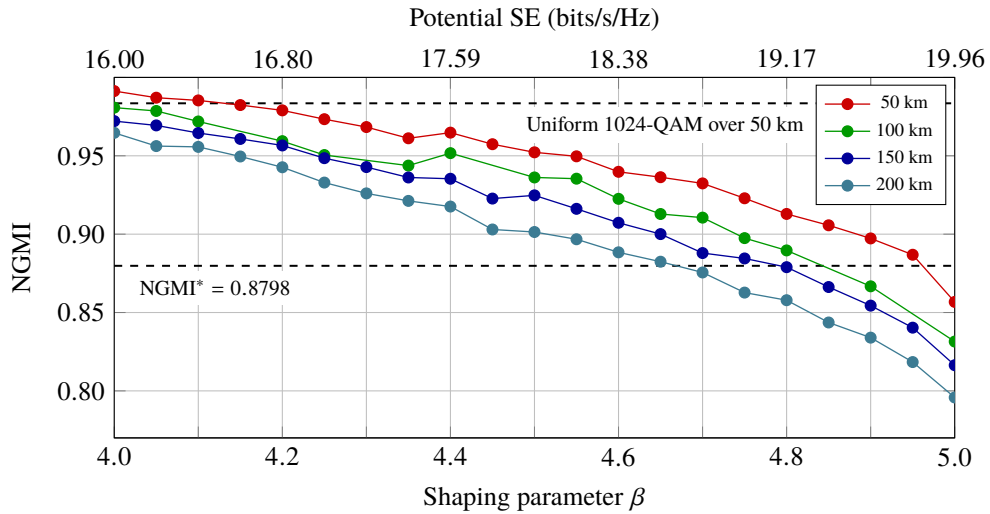


Fig. 5. Measured 3-GBd PS 4096-QAM NGMI versus shaping parameter β . Potential SE takes into account a 19.02% FEC overhead and an RRC roll-off of 0.01.

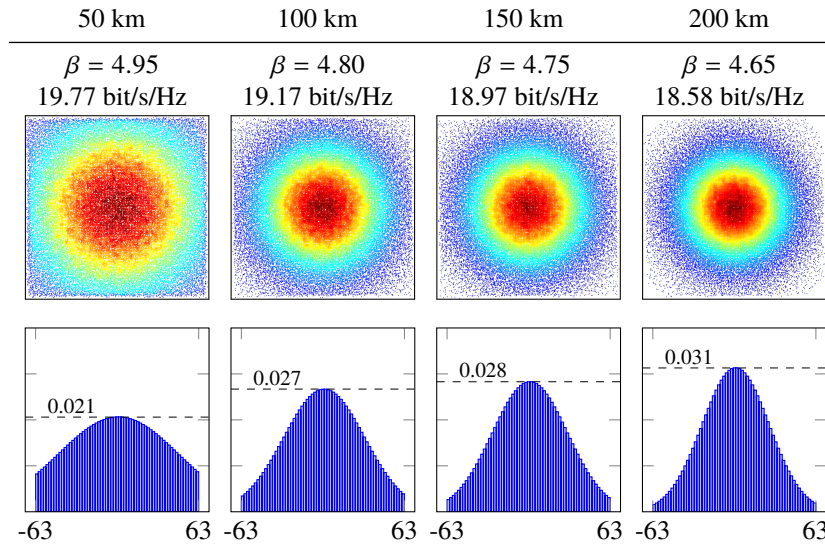


Fig. 6. Top row: Recovered 3-GBd PS 4096-QAM constellation diagrams (x-polarization) for various transmission distances with the largest possible shaping parameters providing a measured NGMI still larger than or equal to the NGMI threshold, i.e., $NGMI \geq NGMI^* = 0.8798$. Bottom row: Histogram of the real part of transmitted signal (x-polarization).

launch powers the signal is distorted by fiber nonlinearities. However, across a wide range of launch powers between -14 dBm and -4 dBm, the system shows a saturated maximum SNR; we therefore picked -9 dBm for the launch power at the center of the saturation region. A typical recovered constellation diagram of the 1024-QAM signal at the saturated SNR is shown in the inset in Fig. 4(b).

Figure 5 shows the measured NGMI for a 3-GBd PS 4096-QAM signal transmitted over 50, 100, 150, and 200 km with various shaping parameters β at -9 dBm launch power. $\beta = 5$

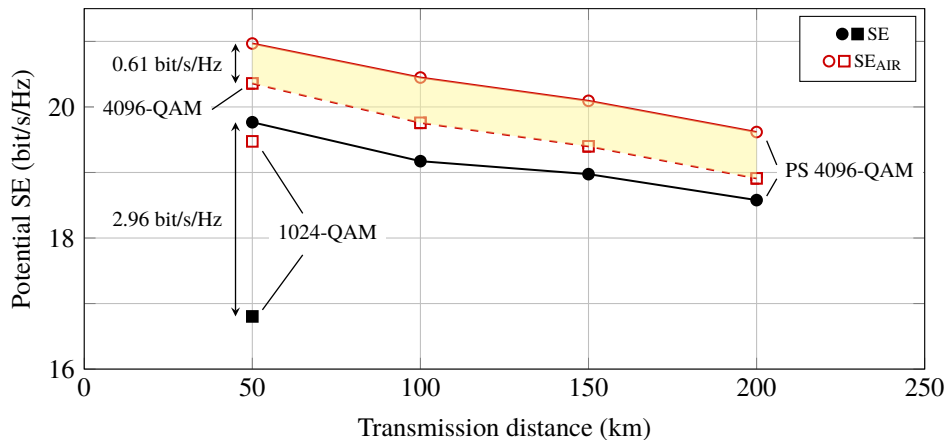


Fig. 7. Measured potential SE versus transmission distance. SE_{AIR} denotes measured AIR scaled by the ratio of the symbol rate (3 GBd) to the signal bandwidth (3.03 GHz), as a measure for achievable performance with ideal FEC.

corresponds to un-shaped uniform 4096-QAM. The potential SE, taking into account the 19.02% FEC overhead and an RRC roll-off of 0.01, is shown on the top horizontal axis. For all four transmission distances the NGMI is reduced as the shaping parameter is increased, as expected. The NGMI for uniform 1024-QAM transmitted over 50 km of fiber at -10 dBm launch power was 0.9835 and is shown in Fig. 5 by the top dashed horizontal line. The largest shaping parameters for PS 4096-QAM providing $NGMI \geq NGMI^*$ and the corresponding potential SEs are summarized in Fig. 6. Also shown in Fig. 6 are histograms of the transmitted signals that led to the maximum potential SE for each distance. Even at the longest transmission distance, the shaping is weak enough to make the constellation extend to the edges of the 4096-QAM modulation template.

From Fig. 5 we see that with the FEC code that we employ in the experiment, uniform 1024-QAM has a large margin of 0.1037 to the NGMI threshold, while uniform 4096-QAM ($\beta = 5$) does not meet the FEC requirement for error-free decoding. Probabilistic shaping over the 4096-QAM constellation template, however, enables us to adjust this margin by tuning the shaping parameter, and we can therefore obtain significantly higher potential SEs than with uniform 1024-QAM while at the same time recovering the data with a post-FEC BER below 10^{-15} .

Figure 7 shows the potential SE versus transmission distance for uniform 1024-QAM (solid black square) and PS 4096-QAM (solid black circles), also shown in Fig. 1. No SE data is shown for uniform 4096-QAM since error-free decoding was not possible using our 0.8402-rate code. To recover the data a lower-rate code (larger overhead) would be needed which would substantially reduce the SE. Comparing the SE of uniform 1024-QAM and PS 4096-QAM at a transmission distance of 50 km shows that PS 4096-QAM increases the potential SE by 2.96 bit/s/Hz, as indicated in the figure. This increase is largely due to rate adaptation and partly due to enhanced energy efficiency (i.e., due to shaping gain). The shaping gain separated from the rate-adapting gain is better shown by the AIR, which assumes an ideal and continuously rate-adaptable FEC. The potential SEs obtained through the AIR instead of a realistic FEC is shown in Fig. 7 for uniform 1024-QAM (open square), PS 4096-QAM (open circles), and uniform 4096-QAM (open squares). The AIR is scaled by the ratio of the symbol rate (3 GBd) to the signal bandwidth including the RRC roll-off (3.03 GHz) to obtain a metric that is easily comparable to the potential SE. We denote the scaled AIR by SE_{AIR} . By comparing the SE_{AIR} for PS 4096-QAM to the SE_{AIR} for uniform 4096-QAM we can extract the shaping gain provided by PS 4096-QAM. The

shaping gain (yellow highlighted region) amounts to 0.61 bit/s/Hz at 50 km transmission and is roughly the same over all measured transmission distances.

5. Conclusion

We have demonstrated transmission of 3-GBd PS 4096-QAM over up to 200 km of backward Raman amplified Vascade EX2000 fiber showing a potential SE of 19.77 bit/s/Hz and a net bit rate of 59.89 Gb/s over 50 km of fiber (18.58 bit/s/Hz at 56.29 Gb/s over 200 km). The improvement in potential SE using PS 4096-QAM compared to using uniform 1024-QAM with our code rate of 0.8402 originates mainly from rate-adaptation but also from shaping gain, i.e., enhanced energy efficiency. Slightly reduced SEs are expected in a realistic WDM scenario where a guard band of ~5% of the symbol rate is typically required.